IOSR Journal of Applied Physics (IOSR-JAP)
e-ISSN: 2278-4861.Volume 9, Issue 4 Ver. IV (Jul. – Aug. 2017), PP 44-51
www.iosrjournals.org

Theoretical Study of Fiber Laser Based On Thulium-Doped Silica Fiber

[*]Muhssen Salbookh Erhayief,
Mustansiriyah University
Corresponding Author: Muhssen Salbookh Erhayief

***Abstract**: In this research the study of fiber laser depends on an analytical theory which is including a three-level laser system. Any increased in core radius and pump power means increased in output power for optimum core radius3.8μm we get 25mW output power. Optimum length depends on pumping power. Any increase in fiber length causes increasing in output power.*

Date of Submission: 02-08-2017 Date of acceptance: 25-08-2017

I. Introduction

The pulse propagation in optical fiber suffers many losses which causes attenuation to the propagated pulse after passing several kilometers, therefore fiber laser should be use to raise the power level of the attenuated pulse [1]. Most fiber laser amplify incident light through stimulated emission, the same mechanism that is used by normal lasers. Its main ingredient is the output power realized when the amplifier is pumped (optically or electrically) to achieve population inversion [2]. The output power, in general, depends not only on the frequency (or wavelength) of the incident signal, but also on the local beam intensity at any point inside the amplifier. Details of the frequency and intensity dependence of the output power depend on the fiber laser medium. The optimization of the fiber length, core radius for a Th^{3+} doped fluorozirconate fiber laser operating at 1550nm wavelength will be presented [3,4]. Many advantages of fiber lasers stem from the collinear confinement of the pump and signal beams to the same small core region of the optical fiber where they can interact for long distances (many tens of meters). Because of the small core radius of the doped fiber, a lower pumping power may be required [5,6].

II. Theoretical Treatment:

A three level rate-equation model commonly used for lasers can be adapted for Thulium doped fiber laser TDFL. It is sometimes added a fourth level to include the excited-state absorption, but that is valid when ASE and excited-state absorption are negligible. In general, the resulting equations must be solved numerically [7]. Consider the energy levels of a laser system shown in figure 1. N_i is the number of ions per unit volume in level i, the rate equations is given by:

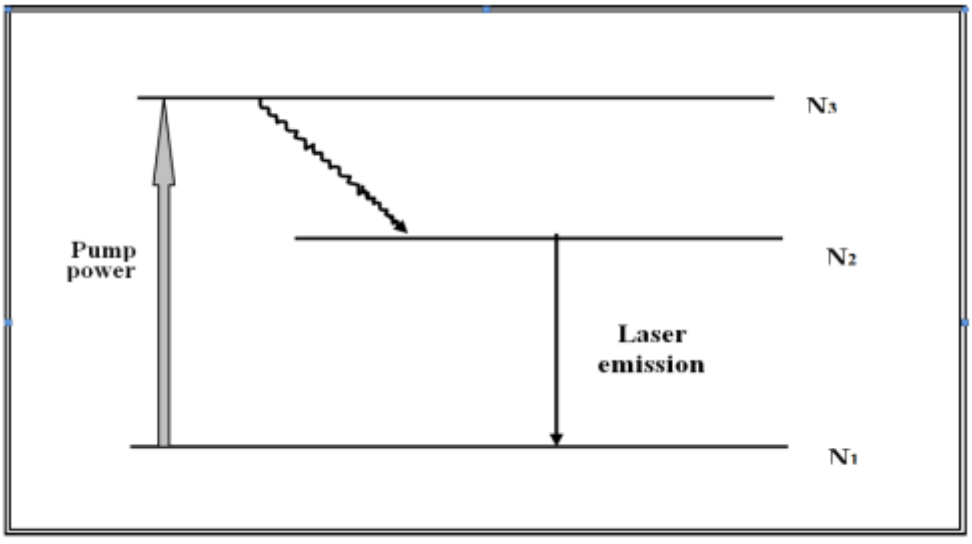

Figure 1 three energy levels of a laser system [8]

Denoting N_i the number of ions per unit volume in level i, the rate equations is given by: [8]

$$\frac{dN_3}{dt} = N_1 w_p - N_3 (x_p w_p + w_3) \quad (1)$$

$$\frac{dN_2}{dt} = N_3 w_{32} + N_1 w_{12}^{\ d} - N_2 (w_2 + w_{21}^{\ d}) \quad (2)$$

$$\frac{dN_1}{dt} = N_3 w_{31} + N_2 (w_{21} + w_{21}^{\ d}) - N_1 (w_{12}^{\ d} + w_1) \quad (3)$$

$$N_o = N_1 + N_{ex} \quad (4)$$

$$N_{ex} = N_2 + N_3 \quad (5)$$

where w_{ij} is the probability per unit time that an ion in level i decays spontaneously to level j (either radiatively or nonradiatively), w_i is the total spontaneous decay rate from level i and w^d_{ij} is the transition rate from level i to level j induced by stimulated emission or absorption, N_o is the total number of ions per unit volume, and N_{ex} is the total population in the excited states.

The pump rate w_P is related to the pump cross section σ_P by: [9]

$$w_p = \frac{I_p \sigma_p}{h\nu_p} \quad (6)$$

where I_P is the pump intensity and $h\nu_P$ is the pump photon energy. The

term $x_P w_P$ on the right hand side of equation 1 corresponds to downward-induced transition by the pump beam. If the level i have degeneracies g_i, the ratio of stimulated emission rate to absorption rate for the pump is $x_p \equiv \frac{g_1}{g_3}$. The absorption and stimulated emission of the lasing radiation are related by the degeneracy ratio[10]:

$$x_r = \frac{w_{12}^{\ d}}{w_{21}^{\ d}} = \frac{g_2}{g_1} \quad (7)$$

In solving equations $1 \rightarrow 5$ for the level populations N_i , it is convenient to introduce two types of spontaneous emission branching ratio. First, $\beta_{ij}=w_{ij} / w_i$ is interpreted as the probability that level i relaxes in a single step (either radiatively or nonradiatively) to level j. The second type of branching ratio will be denoted as b_{ij}, which is defined as the probability that level i relaxes to level j through any combination of downward–going steps. Both of these branching ratios are defined in the absence of any stimulated emission transitions. The multistep branching ratio b_{ij} can be written in terms of the single–step branching ratios β_{ij} as. [11]

$$b_{ij} = \sum_{k=j}^{i-1} \beta_{ik} b_{kj} \quad (8)$$

where b_{ii}=1. At steady states 1 → 3 can be written:

$$N_1 w_p - N_3 (x_p w_p + w_3) = 0 \quad (9)$$

(10)

$$N_3 w_{32} + N_1 w_{12}^d - N_2 (w_2 + w_{21}^d) = 0 \quad (11)$$

$$N_3 w_{31} + N_2 (w_{21} + w_{21}^d) - N_1 (w_{12}^d + w_1) = 0$$

Using the branching ratio notations equation 9 becomes:

$$N_3 = R_p \tau_3 \quad (12)$$

Equation 2-10 can be written as:

$$N_2 = R_p b_{32} \tau_{flu} - \Delta N \, w_{21}^d \tau_{flu} \quad (13)$$

and equation 2-11 can be written as:

$$N_1 = R_p b_{31} \tau_1 + (1 - b_{21}) w_{21}^d \Delta N \tau_1 = 0 \quad (14)$$

where:

$$\tau_i = \frac{1}{w_i}, \; \Delta N = N_2 - x_r N_1, \; b_{31} = \beta_{31} + \beta_{32} \beta_{21}, \; \tau_2 \equiv \tau_{flu}$$

is the average life time of the excited energy level 2, $w_{21}^d = w^d$, and

$$R_p \equiv N_1 \frac{w_p}{1 + x_p w_p \tau_3} \quad (15)$$

Using equations 13 and 14 the population difference ΔN in terms of the ground state population can be written as.

$$\Delta N = R_p \frac{\tau_a}{1 + w^d \tau_b} \quad (16)$$

where:

$$\tau_a = b_{32} \tau_{flu} - b_{31} \tau_1 x_r \quad (17)$$

$$\tau_b = \tau_{flu} + (1 - b_{21}) x_r \tau_1 \quad (18)$$

When equation 2-16 is combined with equations 12 → 14, the population of each excited state is obtained in terms of the ground state population N_1. Equation 12 becomes:

$$N_3 = N_1 \frac{w_p \tau_3}{1 + x_p w_p \tau_3} \quad (19)$$

Equation 13 becomes:

$$N_2 = \frac{N_1 w_p}{1 + x_p w_p \tau_3} \left(b_{32} \tau_{flu} - \tau_{flu} w_{21}^d \frac{\tau_a}{1 + w_{21}^d \tau_b}\right) \quad (20)$$

Then equation 14 becomes:

$$N_1 = N_1 \frac{w_p}{1 + x_p w_p \tau_3} \left(\tau_1 b_{31} + (1 - b_{21}) w_{21}^d \tau_1 \frac{\tau_a}{1 + w_{21}^d \tau_b}\right) \quad (21)$$

The ground state (G.S) population can be evaluated explicitly by summing the exited state (E.S) populations $N_{ex}= N_2+N_3$, then;

$$N_{ex} = \frac{N_1 w_p}{1 + x_p w_p \tau_3} \left(\tau_e - \tau_{flu} w_{21}^d \frac{\tau_a}{1 + w_{21}^d \tau_b}\right) \quad (22)$$

where

$$\tau_e = \tau_3 + b_{32} \tau_{flu} \quad (23)$$

Then from equation 2-14 can get:

$$N_1 = N_o \frac{1 + x_p w_p \tau_3}{1 + w_p (\tau_{ex}^* + x_p \tau_3)} \quad (24)$$

where:

$$S = w_{21}^d \tau_b = \frac{I}{I_{sat}} \quad (25)$$

$$a_2 = 1 - \frac{\tau_{flu} \tau_a}{\tau_b \tau_e} \quad (26)$$

$$\tau_{ex}^* = \tau_e \frac{1 + a_2 S}{1 + S} \quad (27)$$

$$I_{sat} \equiv \frac{h \nu}{\sigma_{se} \tau_b} \quad (28)$$

In the above equation 25 to 28, I is defined as the total lasing intensity in the doped fiber core, σ_{se} is the stimulated emission cross section for the $2 \rightarrow 1$ lasing transition, and hν is the lasing photon energy. τ^*_{ex} plays the role of an effective relaxation time for the excited states. Equation 24 relates the G.S population N_1 in the small region of the fiber to the pump rate w_P in that same small region, for different position x along the fiber, however, the pump rate and the corresponding ground state population will vary due to absorption of the pump photons. The change in pump intensity with x is determined by [12].

$$dI_p = -I_p(N_1 - x_p N_3)\sigma_p dx \qquad 29$$

Using equations 12, 15, and 24, can be written as:

$$dI_p = -I_p \frac{N_o \sigma_p}{1 + w_p(\tau^*_{ex} + x_p \tau_3)} dx \qquad 30$$

If the lasing intensity varies with position along the fiber, τ^*_{ex} is varied also. In a fiber laser, however, it is often the case that the lasing intensity varies only slightly with position along the fiber. Equation 2-30 can be integrated, yielding:

$$\ln\left(\frac{I_p}{I_{po}}\right) + \frac{\sigma_p(\tau^*_{ex} + x_p\tau_3)}{h\nu_p}(I_p - I_{po}) = \alpha_p L \qquad 31$$

where I_{p_o} and I_p are the pump intensities at the beginning (x=0) and end (x=L) of the fiber, respectively, and $\alpha_p \equiv N_o\,\sigma_p$ is the low intensity pump absorption coefficient.

III. Result And Discussion

Analysis of variation of output power based on some parameters such as concentration, core radius, fiber length and pump power will be numerically discussed. The following data that are used in simulation program for Thulium doped fiber lasers, N_A =0.15, α_L=2.3×10^{-4}cm^{-1}, τ_2= 5.64mS, τ_3= 1.36mS, W_{32}= 24S^{-1}, β_{32}=0.033, W^{d}_{32} = 24S^{-1}, X_r= 9/11, X_P=3/9, λ_P= 790nm, λ_s= 2.3 μm, σ_P=3.44×10^{-21} cm^2, σ_{se}=3.3×10^{-21}cm^2 [27,50,51].

Figure 2 shows the effect of the variation of the concentration on the output power. Any increasing in doping concentration means leaner increasing in the output power and the change in the pump power (10, 20 and 30mW) also means increasing in output power. Plotting the output power versus fiber lengths with different pump power of Th^{3+} doped fiber is shown in figure 3. As expected, longer fibers are able to produce a higher output power because it can absorb a great pump power. The maximum output power scale linearly with fiber length. The effects of variation of pump power (5, 10 and 15mW) on the output power are shown in figure 3, where any increase in fiber length and pump power causes increasing in output power. Figure 4 is explained an exponential relation between output power and pump power for different lengths, as it clear any increase in fiber length means higher output power, In order to keep the amplifier as short as possible, though with a good efficiency, one could think that highly doping concentration is the best. Figure 5 shows output power as a function of core radius at different pump power. For any value of pump power, output power is increased with any increase in core radius until optimum value of core radius (of higher\ output power), then output power will be decreased as core radius increase which equal zero at core reduce (3.5,5 and 6μm) for (6,12 and18mW) respectively. Any increased in core radius and pump power means increased in output power. For 18mW pump power there is 25mWof output power at 3.8μm core radius nearly.

Figure 6 shows output power as a function of core radius for different lengths, for all lengths output power is increased with the increasing of core radius until optimum value of core radius (3μm), then output power will be decreased as core radius increase which equal zero at core reduce (4.75μm). But as fiber length is increased (5, 10, and 15m) output power will increase (16, 42 and 68mW).

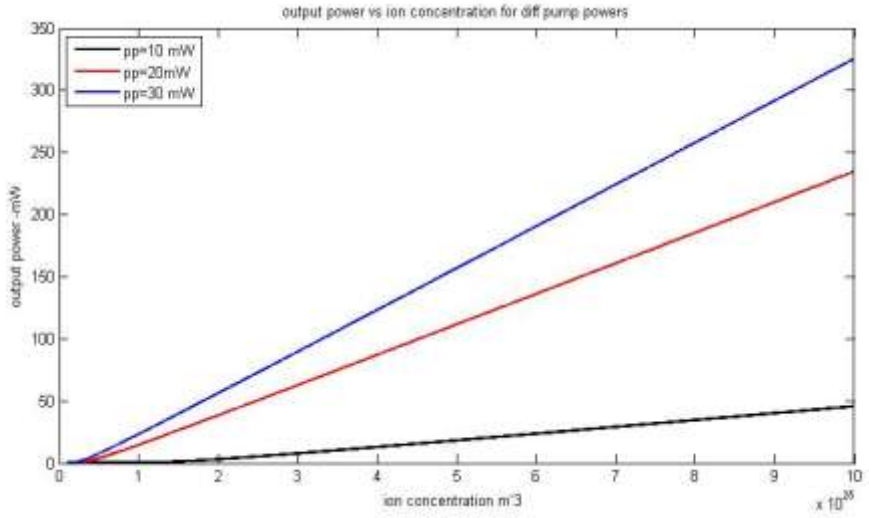

Fig (2): output power vs. ion concentration for diff. pump power of (TDFL) λ_p=790nm, λ_s=2.3μm , l=10m , a= 2μm.

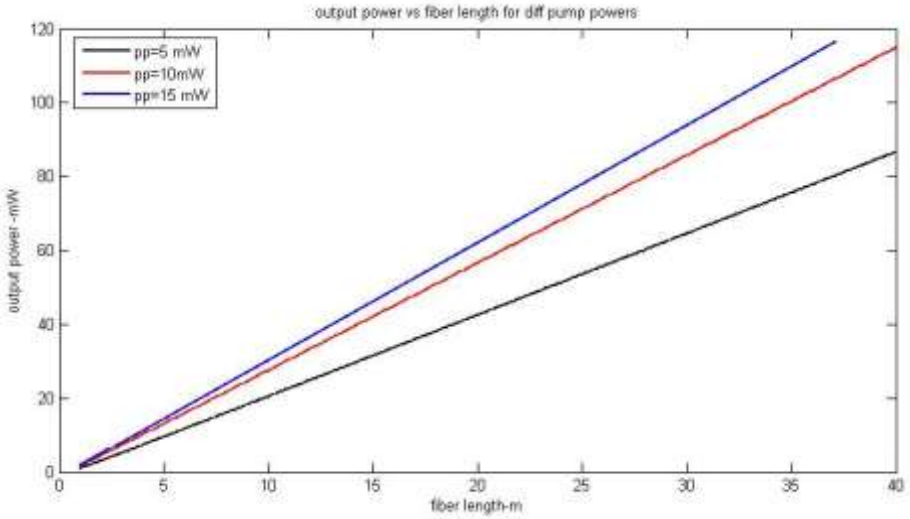

Fig (3): output power vs. fiber length for diff. Pump power of (TDFL) λ_p=790nm, λ_s=2.3μm, a= 2μm, N=4*$10^{25}m^{-3}$.

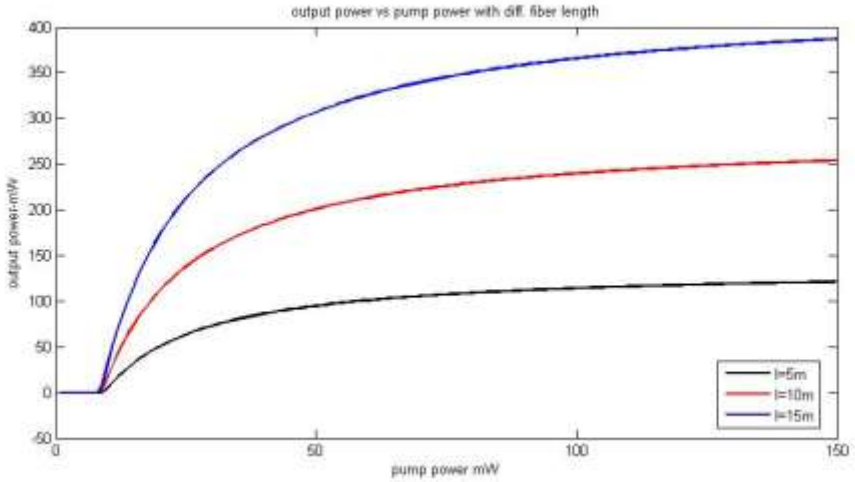

Figure 4: output power vs. Pump power for diff. fiber length of (TDFA) λ_p=790nm, λ_s=2.3μm , a=2μm , N=4*$10^{25}m^{-3}$.

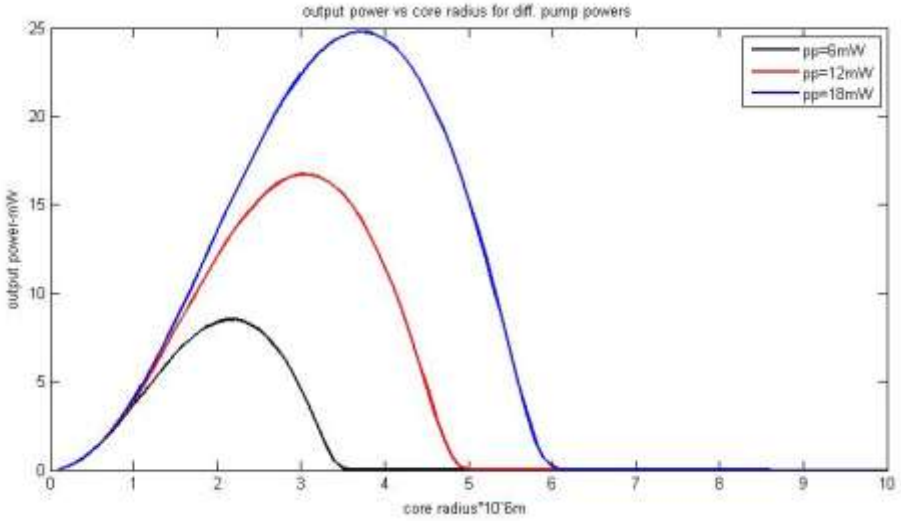

Figure 5: output power vs. core radius for diff. Pump power of (TDFL) λ_p=790nm, λ_s=2.3μm, L=10m, N=4*$10^{25}m^{-3}$.

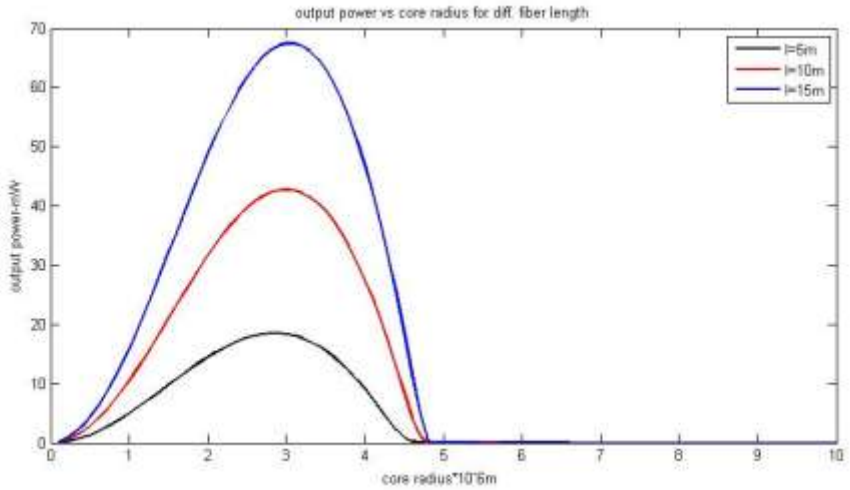

Figure 6: output power vs. core radius for diff. fiber length of (TDFA) λ_p=790nm, λ_s=2.3μm, pp=6mW, N=4*$10^{25}m^{-3}$.

IV. Conclusion

The following conclusions can be drawn:

Longer fiber is able to produce a higher output power because; it can absorb a great of pump power. Large output power for small core radius results in on active fiber device which can combine the excellent properties of standard laser material and the high energy confinement available in optical fiber of small effective area. In order to keep the amplifier as short as possible though with a good efficiency, one could think that the highest doping concentration is recommended.

References

[1]. M. Ming-Kang Lin, "Principles and applications of optical Communications", McGraw-Hill Com. Int., (1996).
[2]. P. Peterka, I. Kasik, B. Dussardier, W. Blanc "Theoretical analysis of fiber lasers emitting around 810 nm based on thulium-doped silica fibers with enhanced 3H4 level lifetime" Author manuscript, published in 4th EPS-QEOD Europhoton Conference, Germany (2010).
[3]. Peng Wan, Lih-Mei Yang and Jian Liu,"156 micro-J ultrafast Thulium-doped fiber laser," SPIE Photonics West (2013).
[4]. S Tessarin, M. Lynch, J.F. Donegan, and G. Mazé," Thulium doped ZBLAN fibre ring-cavity amplifier" Proc. of SPIE Vol. 5825, (2010).
[5]. G. P. Agrawal, "Applications of nonlinear fiber optics", Academic presses, (2001).
[6]. Falah Hassan Abbas "Studying lasers of the single mode optical fibers doped with erbium or thulium" Msc. Thesis, Submitted to Ibn Al-Haitham Collage of Education, University of Baghdad (2008).
[7]. Abdul K. Hussein Dagher ," Semi Classical Analysis of Thulium Doped Optical Fiber Amplifier ,"International Journal of Application or Innovation in Engineering & Management (IJAIEM) Volume 3, Issue 1, January 2014.

[8]. R. Qunimby, "Output saturation in fiber lasers", Appl. Optics, 29, No. 9, p. 1268-1276, 1990.
[9]. W. D. Risk, "Modeling of longitunally pumped solid state lasers exhibiting Re absorption losses", J. Opt. Soc. Am. B, 15, p. 1412-1423, 1988.
[10]. T. Y. Fan and R. L. Byer, "Modeling cw operation of a Quasu-three-level 946nm Nd-YaG laser", IEEE J. Quantum Electron QE, **23**, p. 605-612, 1987.
[11]. N. A. Riza and M. J. Mughal, "Broadband optical equalizer using fault tolerant digital micromeres", International Electron J. Optic., **11**, p. 1559-15565, 2003.
[12]. Z. Drozowicz, R. J. Temkin, and B. Lax, "Laser pumped molecular lasers", IEEE J. Quantum electronics, QE-**15**, No. 3, p. 170, 1979.

Muhssen Salbookh Erhayief. "Theoretical Study of Fiber Laser Based On Thulium-Doped Silica Fiber." IOSR Journal of Applied Physics (IOSR-JAP) , vol. 9, no. 4, 2017, pp. 44–51.